IL NUOVO CIMENTO Vol. 34 C, N. 2 Marzo-Aprile 2011
DOI 10.1393/ncc/i2011-10833-x

Colloquia: WISH2010

Hadronic and electromagnetic probes of hot and dense matter in a Boltzmann+hydrodynamics model of relativistic nuclear collisions

E. Santini(1), B. Bäuchle(1)(2), H. Petersen(3), J. Steinheimer(1), M. Nahrgang(1) and M. Bleicher(1)(2)

(1) *Institut für Theoretische Physik, Goethe-Universität - Max-von-Laue-Str. 1 D-60438 Frankfurt am Main, Germany*
(2) *Frankfurt Institute for Advanced Studies (FIAS) - Ruth-Moufang-Str. 1 D-60438 Frankfurt am Main, Germany*
(3) *Department of Physics, Duke University - Durham, NC 27708, USA*

(ricevuto l' 11 Ottobre 2010; approvato il 30 Novembre 2010; pubblicato online il 22 Marzo 2011)

Summary. — We present recent results on bulk observables and electromagnetic probes obtained using a hybrid approach based on the Ultrarelativistic Quantum Molecular Dynamics transport model with an intermediate hydrodynamic stage for the description of heavy-ion collisions at AGS, SPS and RHIC energies. After briefly reviewing the main results for particle multiplicities, elliptic flow, transverse momentum and rapidity spectra, we focus on photon and dilepton emission from hot and dense hadronic matter.

PACS 24.10.Lx – Monte Carlo simulations (including hadron and parton cascades and string breaking models).
PACS 25.75.-q – Relativistic heavy-ion collisions.
PACS 25.75.Dw – Particle and resonance production.
PACS 25.75.Cj – Photon, lepton, and heavy quark production in relativistic heavy ion collisions.

1. – Introduction

The investigation of nuclear matter under extreme conditions is one of the major research topics of nuclear and high-energy physics. Experimental information about the properties of hot and dense strongly interacting systems is sought by analysing high energy collisions of heavy nuclei. To link specific experimental observables to the different manifestations and, eventually, phases of the strongly interacting matter, a detailed understanding of the dynamics of the heavy-ion reactions is essential.

Numerous observables, such as hadronic and electromagnetic probes, their dynamical pattern and some specific correlations they exhibit, have been and are currently

investigated in detail experimentally. All these observables are generally connected in a non-trivial way. A challenging task, in this respect, is a meaningful modelling of the heavy ion collision. Microscopic (transport) and macroscopic (hydrodynamical) models attempt to describe the full time evolution of the heavy-ion reactions and have played, in their various realizations, an important role in the interpretation of the experimental results over the last decades.

Recently, a third class of models, the so-called "hybrid approaches", has been developed. Hybrid approaches combine the advantages of transport approaches that are well suited to deal with the non-equilibrium initial and final states, with those of an intermediate hydrodynamic evolution, where, *e.g.*, the equation of state (EoS) is an explicit input and phase transitions can be easily implemented. Such approaches were proposed 10 years ago [1, 2] and have since then been employed for a wide range of investigations [3-6]. The hybrid approach discussed here is based on the integration of a hydrodynamic evolution into the Ultra-relativistic Quantum Molecular Dynamics (UrQMD) transport approach [7]. This integrated hybrid approach, called UrQMD v3.3([1]), has been applied by the Frankfurt group to the investigation of various hadronic observables in the broad energy range from $E_{\rm lab} = 2$–$160\,\mathrm{GeV}$ [8-13] and, recently, of electromagnetic probes (photons and dileptons) [14-18], which have the unique feature of being sensible to the *whole* time evolution of the system. Note that in the hybrid model emission of virtual and real photons from the QGP phase can be explicitly accounted for provided that an EoS with a QGP phase is used for the hydrodynamical evolution. This constitutes a great advantage with respect to the pure hadronic transport models, where such emission cannot be easily implemented. In this proceeding, we briefly survey some of the results obtained both for the hadronic and electromagnetic sector.

2. – A hybrid approach to heavy-ion collisions

Hybrid models generally schedule three dynamical stages: during the initial stage a microscopic transport scheme carries the incidentally colliding nuclei towards a stage that determines the initial conditions for the relativistic hydrodynamic equations of motion. At this stage one assumes local equilibration and the fireball is subsequently followed by a hydrodynamic evolution until the description is handed over to a final-state kinetic transport description. This late stage automatically furnishes a continuous freeze-out process, an important improvement compared to the otherwise employed prescription of an instantaneous freeze-out. Below, we want to briefly summarize the specific realization of the hybrid approach by the Frankfurt group and refer the reader to [7] for further details.

During the first stage of the evolution the particles are described as a purely hadronic cascade within UrQMD. The coupling to the hydrodynamical evolution proceeds when the two Lorentz-contracted nuclei have passed through each other. At this time, the spectators continue to propagate in the cascade and all other hadrons are mapped to the hydrodynamic grid. Subsequently, a $(3 + 1)$ ideal hydrodynamic evolution is performed using the SHASTA algorithm [19, 20]. The hydrodynamic evolution is later merged into the hadronic cascade. Two possible transition criteria procedures were tested. The first is the isochronous freeze-out (IF). In this approach, all hydrodynamic cells are mapped onto particles at the same time, once the energy drops below five times the ground-state

([1]) Website of the UrQMD Collaboration `http://urqmd.org`.

energy density in all cells. The second criterium is called gradual freeze-out (GF). In this approach transverse slices, of thickness 0.2 fm, are transformed to particles whenever in all cells of each individual slice the energy density drops below five times the ground-state energy density. The employment of such gradual transition allows to obtain a rapidity-independent transition temperature without artificial time dilatation effects [21]. When merging, the hydrodynamic fields are transformed to particle degrees of freedom via the Cooper-Frye equation. The created particles proceed in their evolution in the hadronic cascade where final state interactions and decays of the particles occur within the UrQMD framework.

3. – Hadronic probes: a brief review

Compared to treatments solely throughout by kinetic transport, as, *e.g.*, by UrQMD, such hybrid strategies provide a well-pronounced sensitivity of the transverse flow on the hydrodynamic part of the evolution [9, 11, 15]. Among others, they enhance the production of strange particles [8, 12]. In fig. 1, the excitation functions of the Λ, Ξ, Ω, π, K and p yields [22] are shown. The enhancement of the multiplicities for all particles with strange content compared to the non-hybrid results (dotted lines) can be clearly observed.

Investigations of the longitudinal dynamics via rapidity distributions of various hadron species have shown that the latters are not too sensitive to the details of the dynamics for the hot and dense stage [8]. The rapidity distributions for, *e.g.*, π^- and K^+ at three different energies ($E_{\rm lab} = 11, 40$ and $160\,A$ GeV) have been analysed in ref. [8], where it was shown that the general shape of the distribution resulting in the hybrid approach is very similar to the one obtained by pure cascade calculations and in line with the experimental data [23, 24].

An additional outcome of such models is that elliptic flow is found to increase towards collider energies [13] compared to pure cascade calculations.

4. – Electromagnetic probes

Electromagnetic probes, such as photons and lepton pairs, are penetrating probes of the hot and dense matter. Once created these particles pass the collision zone essentially without further interaction and can therefore mediate valuable information on the electromagnetic response of the strongly interacting medium.

In the hybrid approach, emission of real and virtual (dileptons) photons is treated as follows. During the locally equilibrated hydrodynamic stage the production of lepton pairs and direct photons is described by radiation rates for a strongly interacting medium in thermal equilibrium (the so-called "thermal" photons and dileptons). In the evolution stage that precedes or follows the hydrodynamical phase, the emission is performed as typically done in cascade approaches. More specifically, dileptons emission is calculated employing the time integration method that has long been applied in the transport description of dilepton emission (see, *e.g.*, [35]), whereas direct photon emission is calculated according to cross-sections for direct photon production from various channels. We will briefly discuss the main aspects of photons and dilepton emission in the hybrid approach here below. For further detail, the reader is referred to [14, 15, 18].

4˙1. *Photons.* – The most important hadronic channels for the production of direct photons are $\pi\pi \to \gamma\rho$ and $\pi\rho \to \gamma\pi$ [36], which both are implemented in the transport,

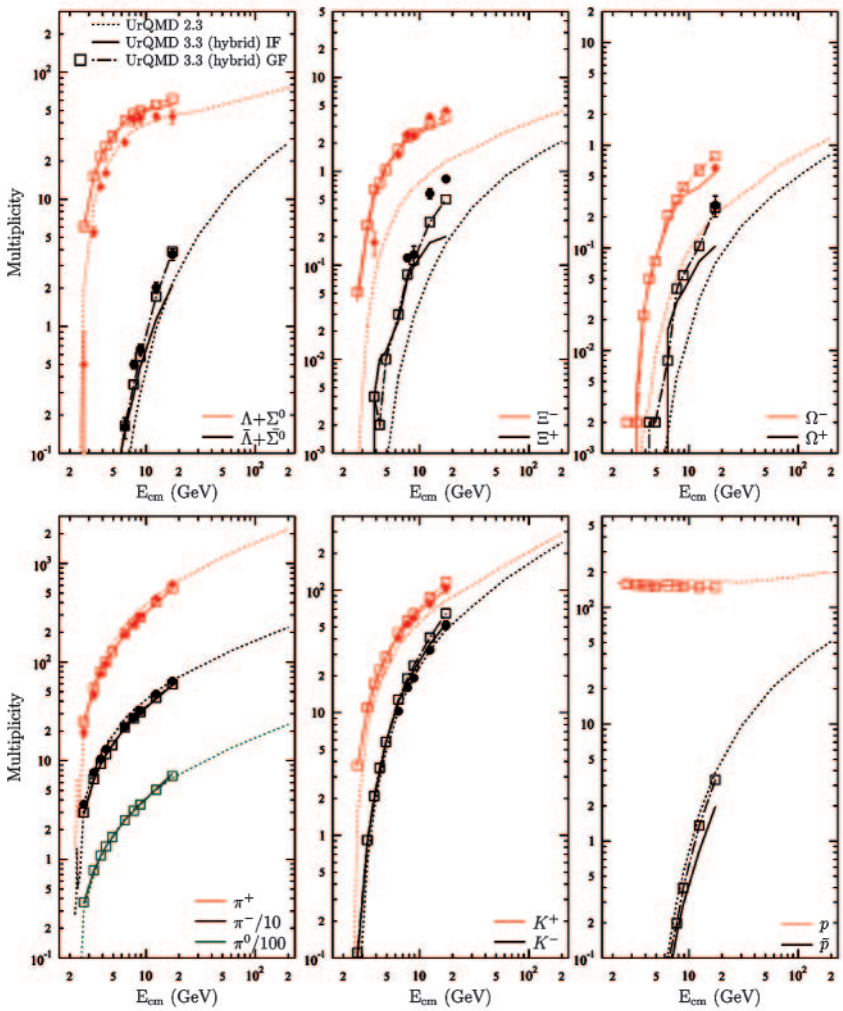

Fig. 1. – (Color online) Excitation functions of the Λ, Ξ, Ω, π, K and p multiplicities (4π) in central ($b < 3.4\,\mathrm{fm}$) Au + Au/Pb + Pb collisions. The results for the hybrid model with isochronous freeze-out (full lines), the hybrid model with gradual freeze-out (squares) and pure UrQMD-2.3 (dotted lines) are compared to experimental data (full symbols) from various experiments [25-34, 24].

as well as in the hydrodynamic phase. The cross-sections for cascade-calculations are taken from Kapusta *et al.* [36], while the rates used for the hydrodynamic description have been parametrized by Turbide *et al.* [37]. Since no thermal partonic interactions are modelled in UrQMD, emission from a QGP-medium is only taken into account in the hydrodynamic part of the model. Several minor hadronic channels are only implemented in one of the two models, such as strange channels (*e.g.*, $K\pi \to \gamma K^*$) which are only present in the hydrodynamic calculations, and η-channels (*e.g.*, $\pi\eta \to \gamma\pi$) which are only present in the transport calculations. Earlier investigations with this model have shown those channels to provide only minor contributions to the overall spectrum

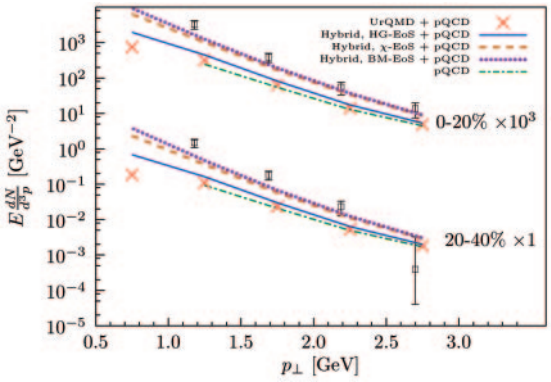

Fig. 2. – (Color online) Comparison of direct photon spectra (open squares) for central (0–20%) and mid-central (20–40%) Au-Au collisions at $\sqrt{s_{NN}} = 200\,\mathrm{GeV}$ [39] to different calculations: a) cascade (red crosses), b) hybrid model with HG-EoS (blue solid line), c) χ-EoS (orange dashed line), and d) BM-EoS (violet dotted line). The contribution from initial pQCD-scatterings [40, 39] has been added to all spectra. The spectra from central collisions have been scaled by a factor of 10^3 to enhance readability.

of direct photons. In the Quark-Gluon-Plasma, the rate used is taken from ref. [38], where convenient parametrizations for the contribution of $2 \leftrightarrow 2$, bremsstrahlung- and annihilation-processes are given. The complete list of channels and a detailed explanation of the calculation procedure is provided in [14].

In fig. 2 a comparison between direct photon spectra from hybrid model calculations and data from the PHENIX Collaboration [39] for central (0–20%) and mid-central (20–40%) Au + Au collisions at $\sqrt{s_{NN}} = 200\,\mathrm{GeV}$ is shown. The experimental data were obtained by extrapolating the dilepton yield to zero invariant mass [39]. The hybrid model calculations were performed using a hadron gas EoS describing a non-interacting gas of free hadrons [41] (HG-EoS, blue solid lines), a chiral EoS that follows from coupling a chiral hadronic $SU(3)$ Lagrangian with a PNJL-type quark-gluon description [42] (χ-EoS, orange dashed lines), and bag model EoS that exhibits a strong first-order phase transition between a Walecka-type hadron gas and massless quarks and gluons [20] (BM-EoS, violet dotted lines). Pure cascade calculations are indicated by red crosses. All calculated spectra include the $\langle N_{\mathrm{coll}} \rangle$-scaled prompt photon contribution taken from [40, 39]. We observe that in both centrality-bins, the direct photon spectra obtained with the BM-EoS and χ-EoS, which include a phase transition to a deconfined state of matter, are significantly higher than the hadronic HG-EoS-calculations. Similar enhancement of photon production due to QGP emission was found already at SPS energies [14].

4˙2. *Dileptons.* – Invoking vector meson dominance the emission rate of lepton pairs from a strongly interacting medium can be related, at low invariant masses, to the spectral properties of the vector mesons, with the ρ meson giving the dominant contribution. The thermal dilepton rate reads then [43]

$$\frac{\mathrm{d}^8 N_{ll}}{\mathrm{d}^4x \mathrm{d}^4q} = -\frac{\alpha^2 m_\rho^4}{\pi^3 g_\rho^2} \frac{L(M^2)}{M^2} f_B(q_0; T)\, \mathrm{Im}\, D_\rho(M, q; T, \mu_B), \tag{1}$$

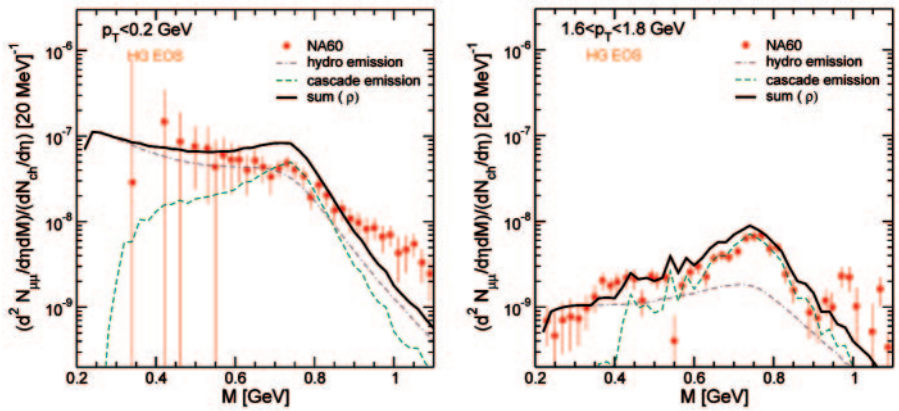

Fig. 3. – (Color online) Left panel: acceptance-corrected invariant mass spectra of the excess dimuons in In-In collisions at 158 A GeV for transverse pair momenta $p_T < 0.2$ GeV, compared to hybrid model calculations based on thermal radiation from in-medium modified ρ meson spectral function (dot-dashed line) and non-thermal cascade emission (dashed line). The sum of the two contributions is depicted by the full line. Experimental data from ref. [49]. Right panel: Same as in the left panel, but for the transverse momenta window $1.6 < p_T < 1.8$ GeV.

where α denotes the fine structure constant, $M^2 = q_0^2 - q^2$ the dilepton invariant mass squared, f_B the Bose distribution function (for a moving fluid this must be substituted with the Jüttner function), and $L(M^2)$ a lepton phase space factor that quickly approaches one above the lepton pair threshold. The electromagnetic response of the strongly interacting medium is then encasted in $\mathrm{Im}\, D_\rho(M, q; T, \mu_B)$, the imaginary part of the in-medium ρ meson propagator,

$$D_\rho(M, q; T, \mu_B) = \frac{1}{M^2 - m_\rho^2 - \Sigma_\rho(M, q; T, \mu_B)}\,. \tag{2}$$

Over the years, strong evidence has been accumulated pointing to the conclusion that the inclusion of the in-medium contributions to the ρ meson self-energy is mandatory for a proper description of the low invariant mass region of the dilepton spectra (see, *e.g.*, ref. [44]), typically characterized by the emerging of an enhancement with respect to the standard hadronic cocktail [45]. A nice aspect of the hybrid approach is that the hydrodynamic stage allows for a transparent inclusion of the in-medium spectral function of the vector meson, conceptually problematic in transport calculations, in analogy to fireball model calculations [46, 47]. An advantage with respect to the latter is the use of a dynamical model for the description of the heavy-ion collisions, which might help to shed some light on dynamical aspects as dilepton radial flow or similar.

In this application, the self-energy contributions taken into account are $\Sigma_\rho = \Sigma^0 + \Sigma^{\rho\pi} + \Sigma^{\rho N}$, where Σ^0 is the vacuum self-energy and $\Sigma^{\rho\pi}$ and $\Sigma^{\rho N}$ denote the contribution to the self-energy due to the direct interactions of the ρ with, respectively, pions and nucleons of the surrounding heat bath. The self-energies have been calculated according to ref. [48], where they were evaluated in terms of empirical scattering amplitudes from resonance dominance at low energies and Regge-type behaviour at high energy.

In fig. 3 hybrid model calculations are compared to recent acceptance-corrected NA60 data [49]. The calculations have been exemplary performed using a hadron gas equation

of state for the hydrodynamical evolution. This is enough to point out qualitatively the main features of the present approach. More systematic studies and discussions will be presented elsewhere [50]. We observe that the cascade emission dominates the invariant mass region around the vector meson peak for both low and intermediate transverse pair momenta p_T. At low p_T (left panel of fig. 3), the very low invariant masses, $M < 0.5\,\mathrm{GeV}$, are filled by the thermal radiation with in-medium spectral function. The sum of both contributions, however, leads to an overestimation of the vector meson peak region at low transverse momenta of the dilepton pair. The reason for the discrepancy might partially lie on the specific spectral function used here and/or, presumably more severely, on the eventual presence of not yet negligible residual in-medium modification of the ρ meson spectral function during the cascade stage, that are here neglected. With increasing p_T (right panel of fig. 3), dilepton emission at very low invariant masses is reduced and the total spectra are almost completely determined by the cascade emission. Indeed, thermal emission had already shown discrepancies for $p_T > 1\,\mathrm{GeV}$ [46], pointing to the necessity to account for non-thermal contributions. In the present approach, the latter appear quite naturally.

Finally, we would like to mention that, in analogy to the direct photons calculations, the present approach easily allows for the inclusion of dilepton emission from QGP, which is thought to play a role in the intermediate mass region of the dilepton spectra.

* * *

ES thanks the organizers for the invitation and for providing partial local support. This work was supported by the Hessen Initiative for Excellence (LOEWE) through the Helmholtz International Center for FAIR (HIC for FAIR) and in part by U.S. department of Energy grant DE-FG02-05ER41367. BB gratefully acknowledges support from the Deutsche Telekom Stiftung, the Helmholtz Research School on Quark Matter Studies and the Helmholtz Graduate School for Hadron and Ion Research. HP acknowledges a Feodor Lynen fellowship of the Alexander von Humboldt foundation. We thank the Center for Scientific Computing for providing computational resources.

REFERENCES

[1] Dumitru A., Bass S. A., Bleicher M., Stoecker H. and Greiner W., *Phys. Lett. B*, **460** (1999) 411.
[2] Bass S. A. *et al.*, *Phys. Rev. C*, **60** (1999) 021902.
[3] Teaney D., Lauret J. and Shuryak E. V., arXiv:nucl-th/0110037, preprint (2001).
[4] Socolowski O. Jr., Grassi F., Hama Y. and Kodama T., *Phys. Rev. Lett.*, **93** (2004) 182301.
[5] Nonaka C. and Bass S. A., *Nucl. Phys. A*, **774** (2006) 873.
[6] Hirano T. and Gyulassy M., *Nucl. Phys. A*, **769** (2006) 71.
[7] Petersen H., Bleicher M., Bass S. A. and Stocker H., arXiv:0805.0567, preprint (2008).
[8] Petersen H., Steinheimer J., Burau G., Bleicher M. and Stocker H., *Phys. Rev. C*, **78** (2008) 044901.
[9] Li Q.-f., Steinheimer J., Petersen H., Bleicher M. and Stocker H., *Phys. Lett. B*, **674** (2009) 111.
[10] Petersen H. and Bleicher M., *Phys. Rev. C*, **79** (2009) 054904.
[11] Petersen H., Steinheimer J., Bleicher M. and Stocker H., *J. Phys. G*, **36** (2009) 055104.

[12] Petersen H., Mitrovski M., Schuster T. and Bleicher M., *Phys. Rev. C*, **80** (2009) 054910.
[13] Petersen H., Steinheimer J., Burau G. and Bleicher M., *Eur. Phys. J. C*, **62** (2009) 31.
[14] Bäuchle B. and Bleicher M., *Phys. Rev. C*, **81** (2010) 044904.
[15] Santini E., Petersen H. and Bleicher M., *Phys. Lett. B*, **687** (2010) 320.
[16] Bäuchle B. and Bleicher M., arXiv:1008.2332, preprint (2010).
[17] Bäuchle B. and Bleicher M., arXiv:1008.2338, preprint (2010).
[18] Santini E. and Bleicher M., arXiv:1009.5266, preprint (2010).
[19] Rischke D. H., Bernard S. and Maruhn J. A., *Nucl. Phys. A*, **595** (1995) 346.
[20] Rischke D. H., Pursun Y. and Maruhn J. A., *Nucl. Phys. A*, **595** (1995) 383.
[21] Steinheimer J., Dexheimer V., Petersen H., Bleicher M., Schramm S. *et al.*, *Phys. Rev. C*, **81** (2010) 044913.
[22] Graf G. *et al.*, *J. Phys. G*, **37** (2010) 094010.
[23] Akiba Y. *et al.*, *Nucl. Phys. A*, **610** (1996) 139c.
[24] Afanasiev S. V. *et al.*, *Phys. Rev. C*, **66** (2002) 054902.
[25] Klay J. *et al.*, *Phys. Rev. C*, **68** (2003) 054905.
[26] Pinkenburg C. *et al.*, *Nucl. Phys. A*, **698** (2002) 495.
[27] Chung P. *et al.*, *Phys. Rev. Lett.*, **91** (2003) 202301.
[28] Alt C. *et al.*, *Phys. Rev. C*, **77** (2008) 024903.
[29] Anticic T. *et al.*, *Phys. Rev. Lett.*, **93** (2004) 022302.
[30] Mitrovski M. K. *et al.*, *J. Phys. G*, **32** (2006) S43.
[31] Alt C. *et al.*, *Phys. Rev. C*, **78** (2008) 034918.
[32] Blume C., *J. Phys. G*, **31** (2005) S685.
[33] Afanasiev S. *et al.*, *Phys. Lett. B*, **538** (2002) 275.
[34] Alt C. *et al.*, *Phys. Rev. Lett.*, **94** (2005) 192301.
[35] Schmidt K. *et al.*, *Phys. Rev. C*, **79** (2009) 064908.
[36] Kapusta J. I., Lichard P. and Seibert D., *Phys. Rev. D*, **44** (1991) 2774.
[37] Turbide S., Rapp R. and Gale C., *Phys. Rev. C*, **69** (2004) 014903.
[38] Arnold P. B., Moore G. D. and Yaffe L. G., *JHEP*, **12** (2001) 009.
[39] Adare A. *et al.*, *Phys. Rev. Lett.*, **104** (2010) 132301.
[40] Gordon L. E. and Vogelsang W., *Phys. Rev. D*, **48** (1993) 3136.
[41] Zschiesche D., Schramm S., Schaffner-Bielich J., Stoecker H. and Greiner W., *Phys. Lett. B*, **547** (2002) 7.
[42] Steinheimer J., Schramm S. and Stocker H., arXiv:1009.5239, preprint (2010).
[43] Rapp R. and Wambach J., *Adv. Nucl. Phys.*, **25** (2000) 1.
[44] Van Hees H., these proceedings.
[45] Floris M., these proceedings.
[46] van Hees H. and Rapp R., *Nucl. Phys. A*, **806** (2008) 339.
[47] Ruppert J., Gale C., Renk T., Lichard P. and Kapusta J. I., *Phys. Rev. Lett.*, **100** (2008) 162301.
[48] Eletsky V. L., Belkacem M., Ellis P. J. and Kapusta J. I., *Phys. Rev. C*, **64** (2001) 035202.
[49] Arnaldi R. *et al.*, *Eur. Phys. J. C*, **61** (2009) 711.
[50] Santini E. *et al.*, in preparation.